



AKADÉMIAI KIADÓ

Pollack Periodica •
An International Journal
for Engineering and
Information Sciences

17 (2022) 1, 56–61

DOI:

[10.1556/606.2021.00410](https://doi.org/10.1556/606.2021.00410)

© 2021 The Author(s)

ORIGINAL RESEARCH
PAPER



*Corresponding author.

E-mail: ali.al.dabbas@emk.bme.hu



Corrosion of ISG by Mg-Si precipitation in presence of Ankerite

Ali Al Dabbas*  and Katalin Kopecskó

Department of Engineering Geology and Geotechnics, Faculty of Civil Engineering, University of Technology and Economics, Műegyetem rkp 3, 1111, Budapest, Hungary

Received: February 5, 2021 • Revised manuscript received: June 3, 2021 • Accepted: June 8, 2021

Published online: November 3, 2021

ABSTRACT

Contact with groundwater in the disposal geological site will induce the creation of an amorphous corrosion layer on the high-level radioactive glass. This is connected to silicate saturation conditions in the surrounding medium, and it is influenced significantly by geochemical processes in the near-field minerals at that depth. The international simple glass is a six-oxide borosilicate glass that is commonly used in nuclear interest. It is a simple glass generated from its composition to be an international benchmark glass. The results of the standard materials characterization center leaching tests in double deionized water at 90 °C and an initial pH value of 6.3 showed that it reacts with Ankerite for a short period of time. The effect of Ankerite on borosilicate glass durability through magnesium-silicate precipitation has been investigated and confirmed in this study.

KEYWORDS

international simple glass, Mg-Si precipitation, high-level radioactive waste, Ankerite, R7T7 glass

1. INTRODUCTION

The nuclear fuel generated is classified as High-Level radioactive Waste (HLW). The HLW is vitrified and is then discharged into stainless steel canisters as a method of pre-processing, preceding the final disposal of a geologic forming repository deeply during a long-term storage [1–4]. In Hungary, the Boda Claystone at Mecsek site is the candidate host rock of high level radioactive waste [5]. Borosilicate glass, a chemical-durable glass for stabilizing high-level waste by leaching tests for nuclear waste glass corrosion in aquatic environments, is stable against many corrosive parameters, but its durability can be influenced over time by critical extrinsic parameters such as temperature, chemicals, and solvents [6].

Flooding in nuclear waste packs occurs as a result of water diffusion via capillary absorption, which is also a process that influences water diffusion across different rock densities, surface tension, and the angle of contact [7]. Additional criteria should be explored in order to forecast water absorption levels, including the porosity, rhyolitic tuff, and the density of stones [8].

The hydration is due to water diffusion across the glass network and the ion exchange between the positive protons found in the aqueous and the glass alkaline metals, frequently leading to the formation of the surface of an amorphous corrosion layer. In a process defined as a hydrolysis, Ionic-covalent bonds of the most soluble elements in the aqueous solution attack the glass network and a reverse mechanism controlled by pH and temperature will be established if the silica easily dissolved in the aqueous solution can condense as a protective gel layer in the outer shell of the glass [9–11].

The protective gel layer should produce a balancing phase, reducing contact between the glass and the aqueous environment [12–14]. That balance leads to silicate saturation in a solution in which the ultimate silicic acid saturation (H_4SiO_4) occurs. Finally, if the

interventions by iron minerals i.e., Ankerite or other geological factors are not carried out [15–21], the corrosion rate of HLW glass should reach a steady state.

2. MATERIALS

2.1. Ankerite

A natural Ankerite-rich geological sample was employed in this investigation. The sample was crushed into a powder using an electrical mortar grinder of tungsten carbide. The X-ray diffraction measurement proved that the sample is a natural Ankerite including a minor amount of Siderite (Fig. 1).

The iron-rich Dolomites or the iron Dolomites are the most so-called Ankerites. Dolomite-Ankerite is still in a constant transition according to the Fe/Mg ratio. $\text{Fe} > \text{Mg}$ and $\text{Fe} > \text{Mn}$ must be present at Ankerite (application of the rule of the predominance cation with predominance valence in each position). That implies that the host rock of the natural Ankerite can be mostly Dolomite [22, 23].

The powder was then sieved using a 100+120 mesh fraction vibratory strainer and collected the 75–125 μm part of the grain size. The Specific Surface Area (SSA) was measured at $225\text{ cm}^2\cdot\text{g}^{-1}$ using the BET- N_2 approach. A portion with grain size 90 percent below 149.01 μm with an average diameter of 88.91 μm was shown by the Particle Size Analyzer (PSA). For further analytical tests this powdered sample was dried overnight at 105°C . Inductively Coupled Plasma - Optical Emission Spectrometry (ICP-OES) was used for the elemental analysis of this sample. Thermal analysis has been used to assess the total carbon content. Table 1 shows the elemental composition of Ankerite.

2.2. International simple glass

International Simple Glass (ISG) is a borosilicate six oxide glass with the same elemental ratios as SON68 (the inactive

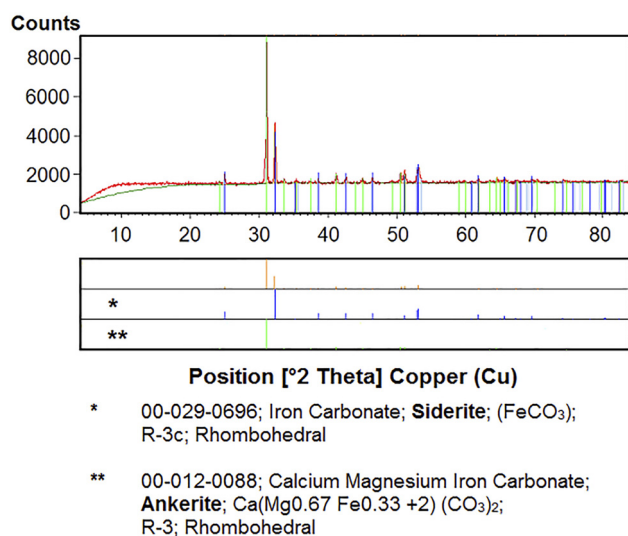


Fig. 1. The XRD pattern of natural Ankerite sample, collected from the mining area in Rudabánya, Hungary

Table 1. Oxide ratios in natural Ankerite, derived from ICP-OES and thermal analysis

Method	Element	Mass (%)	Element	Mass (%)
ICP-OES	SiO_2	0.56	CaO	11.7
	K_2O	0.55	Li_2O	0.03
	Na_2O	0.88	Fe_2O_3	37.6
	Al_2O_3	0.30	MgO	11.9
	MnO	1.18	SO_3	1.50
	CuO	0.53	ZnO	0.03
Method	Element	Mass (%)		
Thermal analysis	CO_2	35.7		
		TOTAL (%)	102.5	

reference glass for the French R7T7 glass). It is commonly used to investigate the HLW glass's durability. The ISG ingot was cut into $10 \times 10 \times 2$ mm plates (coupons) with a diameter of 12.7 cm. The polishing machines using oil-based diamond suspension spray have been used to polish the ISG coupons. Each coupon's Surface Area (SA) was geometrically measured with a digital caliper and found to be 2.4 cm^2 but was adjusted to 3.1 cm^2 after application of a surface roughness factor equal to 1.5 which was calculated using BET- N_2 to account for the additional surfaces. The Inductive Coupling Plasma-Mass Spectrometry (ICP-MS) techniques were used to detect the ISG's composition in percentage ratios. The mass fraction of each element/oxide in the ISG reacted is shown in Table 2.

3. EXPERIMENTAL SETUP AND METHODOLOGY

The commonly performed static leach tests include the standard Materials Characterization Center (MCC) leach test for nuclear waste forms has been established by the U.S. Department of Energy at the Pacific Northwest Laboratory (PNL) [24]. It provides a comparison of the durability of candidate waste forms developed for the stabilization of high-level nuclear wastes [25]. The MCC-1 test has already been standardized by the American Society for Testing and Materials (ASTM) through committee C-26 as Standard C1220-92 [26].

Table 2. Results of the common oxide ratios and mass percentage ratios in ISG

Method	Oxide	Mass (%)	Element	Mole (%)
ICP-OES	SiO_2	55.6	Si	26.0
	B_2O_3	16.0	B	4.61
	Na_2O	13.2	Na	4.91
	Al_2O_3	5.50	Al	1.45
	CaO	5.53	Ca	3.95
	ZrO_2	2.98	Zr	2.21
ICP-MS	Others	<0.79	Others	<0.25
TOTAL (%)		~99.63	~43.38	

The very low Surface area to Volume (S/V) used in the MCC-1 test represents the improbable event of the headspace of a waste canister being instantaneously filled with groundwater and provides a simple method of comparing the relative durability of different homogeneous waste glass. The MCC-1 test is commonly used for low S/V (i.e., $\sim 10 \text{ m}^{-1}$) glass at 90°C . Teflon vessels and ASTM deionized water are required for this test [24].

In the current experiment, the MCC-1 test was employed with PolyTetraFluoroEthylene (PTFE) vessels of a 30 ml capacity each. The leaching was conducted at a temperature of 90°C . The test samples were fabricated by adding specific ($\sim 300 \text{ mg}$) ISG coupons and ($\sim 240 \text{ mg}$) Ankerite powder to the containers, pouring 24 mL of ASTM-I water (having a conductivity and resistivity of $0.055 \mu\text{S}\cdot\text{cm}^{-1}$, $18.2 \text{ M}\Omega\cdot\text{cm}$) in each container, then deoxygenating the samples by Argon gas. The pH of the ASTM-I water was adjusted to 6.3 at 25°C by adding $10 \mu\text{L}$ of $0.08 \text{ g}\cdot\text{L}^{-1}$ NaOH.

Throughout this study, three experimental systems were set up and they were admitted in the oven for (3, 7, 14, 28, 90 days) reacting durations at 90°C :

- System (MCC-1): PTFE vessels were assembled using ISG coupons, each coupon was put into a separate vessel;
- System (reference Ankerite): PTFE vessels were assembled using Ankerite powder. This system was used to facilitate Normalized mass Loss (NL) calculation of dissolved elements, resulting solely from the corrosion product of ISG;
- System (MCC-1 + Ankerite): PTFE vessels were assembled using ISG coupons and Ankerite powder.

At the end of the designated leaching period, the hot samples were cooled to room temperature and then centrifuged at 4,500 rpm for 10 min. The pH value of the leaching solution was measured immediately for all samples at 25°C . pH records are plotted in Fig. 2. The leaching solution was

then filtered through a Millipore filter ($0.45 \mu\text{m}$ pore size) and 15 milliliters of the filtrate were taken for ICP-MS analysis.

4. RESULTS

4.1. Acidity evolution

In the extracted solutions, pH values were shown (Fig. 2) in two ranges:

- pH (7.7–8.3);
- pH (6.2–9.2).

Samples include solely Ankerite powder at 90°C , and samples including Ankerite powder and ISG coupons at 90°C indicate a pH of a range (i). At 90°C the pH values were shown in range (ii) on the reference samples of the glass coupon. Dissolution of Ankerite was found for pH improvements over the first 28 days, which accelerated the ISG corrosion rate [20]. As iron minerals may accelerate their hydrolysis predominantly [27], which will lead to hydroxyl ions being released and H^+ intake from the solution being enhanced [28].

On day 90, and due to the continuous silicate dissolution in the MCC-1 system, an elevation occurred in the pH value, which increased the silicate's solubility while the system was attempting toward saturation. Consequently, the higher pH values on day 90 were eventually attributed to glass corrosion [29]. At the same time, the "MCC-1 + Ankerite" system maintained at steady-state pH after 28 days reaction due to the influence of Ankerite, which regulated the pH and clogged the ISG alteration layer's porosity. This represented a lower rate of ISG corrosion versus MCC-1 as described in Fig. 4.

4.2. Leaching solution analysis

Iron (Fe) concentrations in the ISG systems were lower than the detection limit in the present experiment, which might be owing to its rapid integration into the Si network during the first corrosion phase [16]. Magnesium solubility was observed in various systems. However, lower concentrations in the ISG coupon system were attributable to Mg-Si precipitation, as indicated by the extra silicic acid created as a consequence of increased glass corrosion rates owing to the presence of adequate magnesium in the solution [29].

Due to the development and precipitation of Mg-Si, which may be Sepiolite [30], the main silicic acid concentrations were depleted, and the deficit will be composed of silicic acid provided by glass corrosion. Mg concentrations in the reference Ankerite system achieved a high value on day 90 of this experiment, but the opposite occurred in the "MCC-1 + Ankerite" system. This was due to the initiation of Mg-Si precipitations, which increased silicate solubility as a consequence of the higher pH. The reduced Mg amounts measured at day 90 support this theory (Fig. 3).

The normalized loss (NL_i) was calculated using Eq. (1) [7] for the main elements resulting from the dissolution of

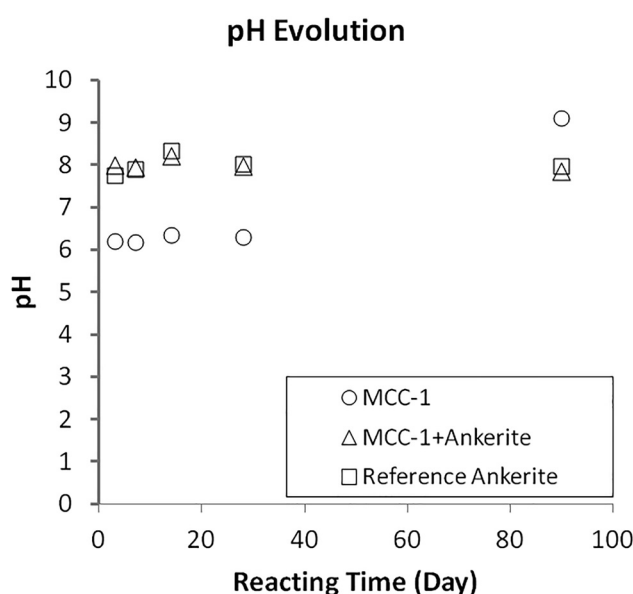


Fig. 2. pH readings for all systems at various leaching times, (point = experiment)



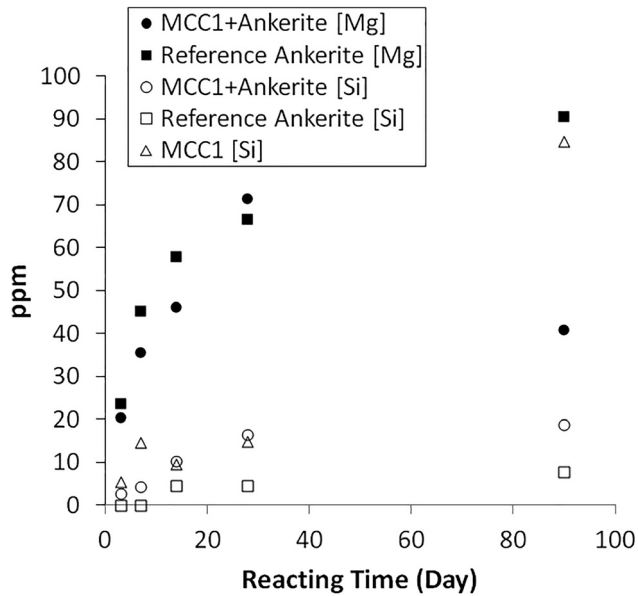


Fig. 3. Evolution of Magnesium and Silicate concentrations with time in all systems, (point = experiment)

the glass samples (Na, B, Si, Ca, Al); concentrations of Zr were not sufficient for said calculations,

$$NL_i = \frac{m_i}{f_i \cdot SA}, \quad (1)$$

where m_i is the mass of element i in the leachate (g); f_i is the mass fraction of element i in the pristine solid (unit less) and SA is the sample geometric surface area (m^2).

Figure 4 depicts the effect of Ankerite by displaying total values of normalized mass loss. The MCC-1 method, however, produced better outcomes. Clogging the porosity of gel [31] was probably mainly due to dissolving products of Ankerite [32]. The normalized weight transfer by a layer that evolves as the glass erodes and/or a rise in glass corrosion product concentrations in the solution; Fig. 4 shows the inverse proportional link between leaching duration and ISG corrosion rate. This reduces the driving force of mass transfer, which slows down the several processes that release these components. The corrosion rate (r) for all leaching methods is shown in Fig. 4 and has been computed by using the following Eqs (2) and (3), used by Neill et al. [15] for ISG:

$$r = \frac{d(E_{th(B)})}{dt}, \quad (2)$$

$$E_{th(B)} = \frac{NL_B}{\rho_{ISG}}, \quad (3)$$

where r denotes the glass corrosion rate ($nm \cdot d^{-1}$); $E_{th(B)}$ is the equivalent thickness of Boron (nm) calculated from the following equation; NL_B is the normalized mass loss for B ($g \cdot m^{-2}$) and ρ_{ISG} is the density of ISG ($2.500 g \cdot cm^{-3}$).

Boron levels were observed to be substantially greater constantly than silicone levels, a typical characteristic concerning corrosion of borosilicate glass. B is, therefore, better

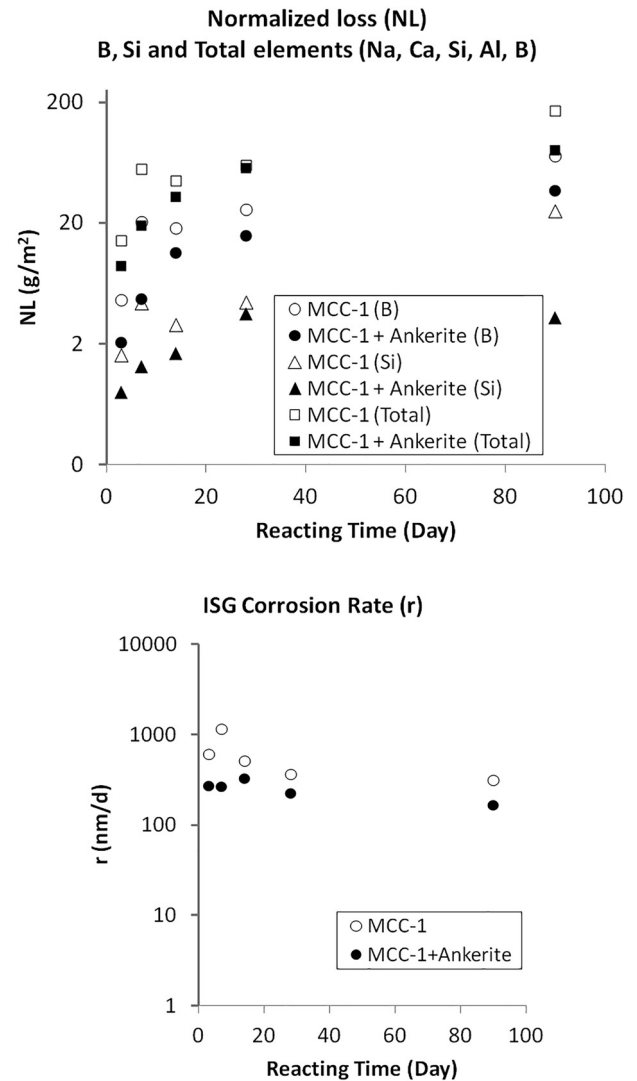


Fig. 4. The main normalized loss results and ISG corrosion rate (r) (point = experiment)

suited to assess glass corrosion rate [29, 33]. Simultaneously, the concentrations of silicon in this study do not apply to the monitoring of glass corrosion because of its constant kinetics and the dissolution/evolution of porous texture in the gel layer [34].

In all systems, the ISG corrosion rate decreased with time (Fig. 4) due to the solution becoming more occupied with glass corrosion products [29]. For the first 14 days of the reaction, the MCC-1 system exhibited the highest corrosion rate and total ISG corrosion products when compared to the “MCC-1 + Ankerite” system. However, on day 90, the “MCC-1 + Ankerite” system began generating Mg-Si precipitations as the silicate solubility increased with increasing the pH.

5. DISCUSSION

In this investigation, iron corrosion products were represented by Ankerite ($CaFe(CO_3)_2$), a common iron carbonate mineral found in soils in various clay matrices [35].



The ISG reference system reached higher corrosion rates and lower pH values during the first 14 days of leaching compared with the Ankerite Mixed System (Fig. 4). At the same time, lower levels of dissolved glass per unit area were exhibited; this is because glass corrosion products are highly concentrated in a solution. ISG glass corrosion rates are reduced by a saturation of the surrounding solution with amorphous silicate (SiO_2). The higher the pH, the higher the silicate in a solution, the higher the pH, the more the pH control was achieved by providing the ideal medium for increased silicate solubility. The gel layer formation was not enough as long as it did not show a substantial reduction in the ISG corrosion rate because of insufficient silicic acid concentration [29].

When Ankerite is present, fewer quantities of boron are released from the glass. Simultaneously, silicon concentrations in MCC-1 systems were much higher. On day 90, they attained a high of (85 mg.L^{-1}) compared to “MCC-1 + Ankerite” (19 mg.L^{-1}) at the same time. As already stated, any silicate consumption in the solution will result in further supplies of silicate from the glass. Sorption and precipitation by Ankerite took place, but the impact of precipitation was nevertheless more substantial since sorption is typically more intense at higher concentrations of silicon acid [36]. Due to the low surface area of ISG to leachate volume, there were not adequate concentrations of silicon acid. The principal concentration of silicic acid is conceivable when the amorphous layer, SiO_2 , begins to disintegrate and dissolve after 90 days of reaction.

In the experiment conducted, NL is a focal factor in the calculation of the glass corrosion rate and is aimed illustrating a better understanding of the normalized elementary loss of the glass components owing to the probable effects of Ankerite on the pH levels. Investigations and analysis of the ICP-MS data show that the released Mg and other corrosion products i.e., Carbonates from Ankerite increased the pH of the leachate in the initial phase of leaching, thereby increasing silicate solubility and initiating early Mg-Si precipitation. However, the presence of Ankerite during the 90 days of reaction was sufficiently effective to reduce ISG's corrosion rates by (i) regulating the pH to not approach free pH value (≈ 9); and (ii) its products of dissolution were able to clog the newly produced gel layer which decreased the exchange with the external area.

6. CONCLUSION

This paper illustrated the results of our research in which the influence of Ankerite, Mg-Si precipitation, on ISG durability during the 90 days of disposal was studied. The dissociation of Silicic acid increased as pH increased, requiring more glass to be dissolved to achieve saturation in solution. In comparison to the pure glass water system, adding Ankerite regulated the pH. Thus, throughout the entire period, Ankerite's pH influence on glass corrosion may explain its impact on glass corrosion. In contrast, the Mg-Si precipitation in Ankerite + ISG system was not aggressive until day 90 of reaction due to

the clogging effect, and the system was attempting toward saturation. Under the present experimental conditions, the pH-profile of Mg-Si precipitation over longer durations should be investigated further.

ACKNOWLEDGEMENT

The Stipendium Hungaricum Scholarship Programme is highly acknowledged for supporting this PhD study and research work. Authors acknowledge the Department of Inorganic and Analytical Chemistry, Faculty of Chemical Engineering, BME for doing the ICP-OES tests on the Ankerite. Authors are grateful for the help of Department of Atomic Physics, Faculty of Natural Sciences, BME in cutting and polishing the ISG glass. This research was also assisted by the Jordan Atomic Energy Commission (JAEC), Jordan Uranium Mining Company (JUMCO) as most of the experimental work and curing was carried out in their laboratories. The authors would also like to acknowledge Savannah River National Laboratory (SRNL), USA, for kindly providing the original ISG sample.

REFERENCES

- [1] IAEA SSR-5 2011, Disposal of Radioactive Waste, Specific Safety Requirements. International Atomic Energy Agency, 2011.
- [2] Andra, *Evaluation of the Feasibility of a Geological Repository in an Argillaceous Formation*. France, Dossier: Report Series, 2005.
- [3] IAEA NW-T-1.19, Geological Disposal of Radioactive Waste: Technological Implications for Retrievability, Nuclear Energy Series, International Atomic Energy Agency, 2009.
- [4] I. Donald, *Waste Immobilization in Glass and Ceramic Based Hosts: Radioactive, Toxic and Hazardous Wastes*. Chichester (UK): Wiley, 2010.
- [5] I. Buocz, N. Rozgonyi-Boissinot, Á. Török, and P. Görög, “Direct shear strength test on rocks along discontinuities, under laboratory conditions,” *Pollack Periodica*, vol. 9, no. 3, pp. 139–150, 2014.
- [6] S. Gin, J. Ryan, S. Kerisit, and J. Du, “Simplifying a solution to a complex puzzle,” *npj Mater. Degrad.*, vol. 2, 2018, Paper no. 36.
- [7] P. Juhász, K. Kopeckó, and Á. Suhajda, “Analysis of capillary absorption properties of porous limestone material and its relation to the migration depth of bacteria in the absorbed biomineralizing compound,” *Periodica Polytechnica, Civil Eng.*, vol. 58, no. 2, pp. 113–120, 2014.
- [8] O. Farkas and Á. Török, “Effect of exhaust gas on natural stone tablets, A laboratory experiment,” *Periodica Polytechnica, Civil Eng.*, vol. 63, no. 1, pp. 115–120, 2019.
- [9] R. Bouakkaz, A. Abdelouas, Y. El Mendili, B. Grambow, and S. Gin, “SON68 glass alteration under Si-rich solutions at low temperature (35–90 °C): kinetics, secondary phases and isotopic exchange studies,” *RSC Adv.*, vol. 6, pp. 72616–72633, 2016.
- [10] H. El Hajj, A. Abdelouas, B. Grambow, C. Martin, and M. Dion, “Microbial corrosion of P235GH steel under geological



- conditions,” *Phys. Chem. Earth, Parts A/B/C*, vol. 35, no. 6–8, pp. 248–253, 2010.
- [11] S. Gin, “Open scientific questions about nuclear glass corrosion,” *Proced. Mater. Sci.*, vol. 7, pp. 163–171, 2014.
- [12] D. Rebiscoul, P. Frugier, S. Gin, and A. Ayrat, “Protective properties and dissolution ability of the gel formed during nuclear glass alteration,” *J. Nucl. Mater.*, vol. 342, no. 1–3, pp. 26–34, 2005.
- [13] E. Vernaz, S. Gin, C. Jegou, and I. Ribet, “Present understanding of R7T7 glass alteration kinetics and their impact on long-term behavior modeling,” *J. Nucl. Mater.*, vol. 298, no. 1–2, pp. 27–36, 2001.
- [14] S. Gin, I. Ribet, and M. Couillard, “Role and properties of the gel formed during nuclear glass alteration: Importance of gel formation condition,” *J. Nucl. Mater.*, vol. 298, no. 1–2, pp. 1–10, 2001.
- [15] L. Neill, S. Gin, T. Ducasse, T. De Echave, M. Fournier, P. Jollivet, and N. A. Wall, “Various effects of magnetite on international simple glass (ISG) dissolution: implications for the long-term durability of nuclear glasses,” *npj Mater. Degrad.*, vol. 1, 2017, Paper no. 1.
- [16] X. Guo, S. Gin, H. Liu, D. Ngo, J. Luo, S. H. Kim, and G. S. Frankel, “Near-field corrosion interactions between glass and corrosion resistant alloys,” *npj Mater. Degrad.*, vol. 4, 2020, Paper no. 10.
- [17] A. A. Dabbas and K. Kopecskó, “Corrosion of glass used for radioactive waste disposal influenced by environmental parameters,” in *Proceedings of the 12th International PhD Symposium in Civil Engineering*, Prague, Czech Republic: Czech Technical University in Prague, August 29–31, 2018, pp. 1071–1078.
- [18] A. A. Dabbas and K. Kopecskó, “Corrosion of glass used for radioactive waste disposal - state of the art,” *Pollack Period.*, vol. 14, no. 1, pp. 85–94, 2019.
- [19] A. A. Dabbas and K. Kopecskó, “Corrosion of glass used for radioactive waste disposal influenced by iron corrosion products,” *IOP Conf. Ser. Mater. Sci. Eng.*, vol. 613, 2019, Paper no. 012030.
- [20] G. Bart, H. Zwicky, E. Aerne, T. Graber, D. Z’berg, and M. Tokiwai, “Borosilicate glass corrosion in the presence of steel corrosion products,” *MRS Online Proc. Libr.*, vol. 84, pp. 459–470, 1986, Paper no. 459.
- [21] M. Debure, P. Frugier, L. De Windt, and S. Gin, “Borosilicate glass alteration driven by magnesium carbonates,” *J. Nucl. Mater.*, vol. 420, no. 1–3, pp. 347–361, 2012.
- [22] K. Krupka, K. Cantrell, and B. McGrail, Thermodynamic Data for Geochemical Modeling of Carbonate Reactions Associated with CO₂ Sequestration - Literature Review, Report no. PNNL-19766. Richland, Washington 99352: Pacific Northwest National Laboratory, 2010.
- [23] R. J. Reeder, “Crystal chemistry of the rhombohedral carbonates,” in *Carbonates: Mineralogy and Chemistry. Reviews in Mineralogy and Geochemistry*, vol. 11, De Gruyter, 1983, pp. 1–47.
- [24] D. Strachan, R. P. Turcotte, and B. O. Barnes, “MCC-1: A standard leach test for nuclear waste forms,” *Nucl. Technol.*, vol. 56, no. 2, pp. 306–312, 1982.
- [25] Nuclear Waste Materials Handbook: Test Methods. Materials Characterization Center. Ser. DOE/TIC-11400, 1981.
- [26] ASMT C1220-92, Standard for Static Leaching of Monolithic Waste Forms for Disposal of Radioactive Waste. Philadelphia, PA: ASTM, 1992.
- [27] B. P. McGrail and K. M. Olson, *Evaluating Long-Term Performance of in Situ Vitrified Waste Forms: Methodology and Results*, Technical Report, Report no. PNL-8358. United States: Pacific Northwest Lab., 1992.
- [28] S. Liu, K. Ferrand, and K. Lemmens, “Transport- and surface reaction-controlled SON68 glass dissolution at 30°C and 70°C and pH=13.7,” *Appl. Geochem.*, vol. 61, pp. 302–311, 2015.
- [29] W. L. Ebert, “The Effects of the Glass Surface Area/solution Volume Ratio on Glass Corrosion: A Critical Review”, Technical Report, Paper no. ANL-94/34. United States: Argonne National Lab., 1995.
- [30] B. Grambow and D. M. Strachan, “Leach testing of waste glasses under near-saturation conditions,” *MRS Online Proc. Libr.*, vol. 26, 1983, Paper no. 623.
- [31] P. Jollivet, F. Angeli, C. Cailleteau, F. Devreux, P. Frugier, and S. Gin, “Investigation of gel porosity clogging during glass leaching,” *J. Non-Crystalline Sol.*, vol. 354, no. 45–46, pp. 4952–4958, 2008.
- [32] A. A. Dabbas and K. Kopecskó, “Corrosion of glass used for radioactive waste disposal influenced by ankerite,” *Advanced Aspects of Engineering Research*. S. M. Lawan, Ed., vol. 9, ch. 10, Book Publisher International, pp. 156–170, 2021.
- [33] W. L. Ebert, and J. J. Mazer, “Laboratory testing of waste glass aqueous corrosion; effects of experimental parameters,” in *Fall Meeting of the Materials Research Society*, Boston, United States, Nov 29 - Dec 3, 1993, Paper no. ANL/CMT/CP-80025.
- [34] S. Gin and P. Frugier, “SON68 glass dissolution kinetics at high reaction progress: experimental evidence of the residual rate,” *MRS Online Proc. Libr.*, vol. 757, 2002, Paper no. II5.9.
- [35] L. Werme, I. K. Björner, G. Bart, H. U. Zwicky, B. Grambow, W. Lutze, R. C. Ewing, and C. Magrabi, “Chemical corrosion of highly radioactive borosilicate nuclear waste glass under simulated repository conditions,” *J. Mater. Res.*, vol. 5, no. 5, pp. 1130–1146, 1990.
- [36] K. Kopecskó and A. A. Dabbas, “Silicate sorption on Ankerite from a standard silicate solution,” *Periodica Polytechnica Chem. Eng.*, vol. 65, no. 3, pp. 400–407, 2021.

